Supplement of Atmos. Chem. Phys., 20, 6725–6747, 2020
https://doi.org/10.5194/acp-20-6725-2020-supplement

Atmospheric Chemistry and Physics
Open Access
EGU

Supplement of

Multiphase MCM–CAPRAM modeling of the formation and processing of secondary aerosol constituents observed during the Mt. Tai summer campaign in 2014

Yanhong Zhu et al.

Correspondence to: Likun Xue (xuelikun@sdu.edu.cn) and Hartmut Herrmann (herrmann@tropos.de)

Table S1. Emission data applied in the SPACCIM (#: anthropogenic emission values, *: biogenic emission values).

Compound	Emission / molec cm^{-3} s^{-1}	Compound	Emission / molec cm^{-3} s^{-1}
Acetone#	3.51E+04	Acetaldehyde#	1.44E+04
Ethane#	1.30E+05	Ethylene#	1.76E+05
Propane#	1.87E+05	Glyoxal#	1.04E+04
n-Butane#	6.79E+04	Formaldehyde#	3.15E+04
Isobutane#	2.99E+04	Biacetyl#	1.49E+03
2,2-Dimethyl Butane#	2.00E+03	Benzaldehyde#	3.37E+02
Isopentane#	6.75E+04	Methacrolein#	2.08E+03
n-Pentane#	2.67E+04	Methyl ethyl ketone#	8.68E+03
2-Methyl Pentane#	1.57E+04	Methanol#	2.28E+04
3-Methylpentane#	1.10E+04	Methylglyoxal#	3.93E+03
n-Hexane#	6.28E+03	Methyl Vinyl Ketone#	2.62E+02
n-Heptane#	4.71E+03	Propene#	2.96E+04
2,3-Dimethyl Butane#	4.71E+03	1-Hexene#	2.45E+04
n-Decane#	1.77E+04	1-Butene#	1.22E+04
3-Methyl Hexane#	1.77E+04	1-Pentene#	1.12E+04
n-Nonane#	6.45E+03	3-Methyl-1-Butene#	3.06E+03
n-Octane#	6.45E+03	cis-2-Pentene#	2.25E+04
2-Methyl Hexane#	4.84E+03	trans-2-Pentene#	2.25E+04
n-Dodecane#	3.22E+03	1,3-Butadiene#	9.64E+03
n-Undecane#	1.61E+03	2-Methyl-2-Butene#	8.03E+03
Toluene#	1.39E+05	Cis-2-Hexene#	8.03E+03
Ethyl Benzene#	1.86E+04	Trans-2-Hexene#	8.03E+03
n-Propyl Benzene#	7.43E+03	Propionaldehyde#	6.40E+03
Isopropyl Benzene#	3.72E+03	Limonene#	3.28E+02
m-Xylene#	1.46E+04	Carbon monoxide#	3.04E+07
p-Xylene#	1.46E+04	Carbon dioxide#	1.15E+09
o-Xylene#	1.23E+04	Ammonia#	3.81E+06
1,2,3-Trimethyl Benzene#	1.01E+04	Nitric Oxide#	2.51E+05
1,3,5-Trimethyl Benzene#	1.01E+04	Nitrogen dioxide#	1.42E+06

m-Ethyl Toluene[#]	5.61E+03	Sulfur dioxide[#]	1.91E+06
o-Ethyl Toluene[#]	5.61E+03	Isoprene[*]	4.05E+05
p-Ethyl Toluene[#]	5.61E+03	a-pinene[*]	2.99E+04
1,2,4-Trimethyl Benzene[#]	5.61E+03	β-pinene[*]	1.28E+04

45

Table S2. Deposition velocities applied in the SPACCIM.

Compound	Deposition / s^{-1}	Compound	Deposition / s^{-1}
Methanol	1.00E-05	N_2O_5	2.00E-05
Carbon monoxide	1.00E-06	Ammonia	1.00E-05
Ethanol	5.00E-06	Nitrogen dioxide	4.00E-06
Hydrogen peroxide	1.00E-05	Ozone	4.00E-06
Formaldehyde	1.00E-05	Formic acid	1.00E-05
Hydrochloric acid	1.00E-05	Sulfur dioxide	1.00E-05
Nitric acid	2.00E-05	Sulfuric acid	2.00E-05

Table S3. Initial gas-phase concentrations applied in the SPACCIM.

Compound	Concentration	Compound	Concentration
Nitric oxide	0.32 ppbv	p-Xylene	94.53 pptv
Nitrogen dioxide	1.72 ppbv	m-Xylene	94.53 pptv
Ozone	100.33 ppbv	Acetaldehyde	1.00 ppbv
Nitric acid	0.67 ppbv	Propionaldehyde	70.48 pptv
Hydrogen peroxide	0.31 ppbv	Butyraldehyde	35.32 pptv
Formaldehyde	0.70 ppbv	Acetone	1.07 ppbv
Hydrogen	0.46 ppmv	Methyl ethyl ketone	29.44 pptv
Carbon monoxide	1.18 ppmv	Methyl isobutyl ketone	13.02 pptv
Methane	2.06 ppmv	Glyoxal	0.21 ppbv
Carbon dioxide	332.10 ppmv	Glycolaldehyde	0.21 ppbv
Sulfur dioxide	2.14 ppbv	Methylglyoxal	18.57 pptv
Ethane	0.43 ppbv	Peroxyacetyl nitrate	92.87 pptv
Propane	80.43 pptv	Methyl hydrogen peroxide	0.19 ppbv

Isoprene	96.19 pptv	Ethyl hydrogen peroxide	18.57 pptv
n-propanol	1.30 pptv	Peroxyacetic acid	0.19 pptv
Isopropanol	51.00 pptv	Ammonia	4.39 ppbv
Butanol	0.75 pptv	Methanol	0.42 ppbv
Isobutanol	0.56 pptv	Ethanol	0.40 ppbv
Ethylene glycol	1.17 pptv	Glyoxylic acid	0.11 ppbv
Ethylene	0.96 ppbv	Glycolic acid	0.11 ppbv
Toluene	0.31 ppbv		
Cresol	0.19 pptv		
o-Xylene	62.61 pptv		

Table S4. Aerosol compositions and parameters applied in the SPACCIM.

Compound	Data / $g_{compound}\ g_{aerosol}^{-1}$	**Parameter**	**Data**
Sulfate	0.25	Aerosol radius	2.0E-07 m
Nitrate	0.21	Aerosol Density	1770 kg m^{-3}
Ammonium	0.16	Aerosol number concentration	5.1E+08 m^{-3}
Water-soluble organic carbon	0.07		
HULIS	0.07		
Water-insoluble organic carbon	0.05		
Positive monovalent ions	0.03		
Positive divalent ions	0.01		
Metals	0.03		
Elemental carbon	0.03		

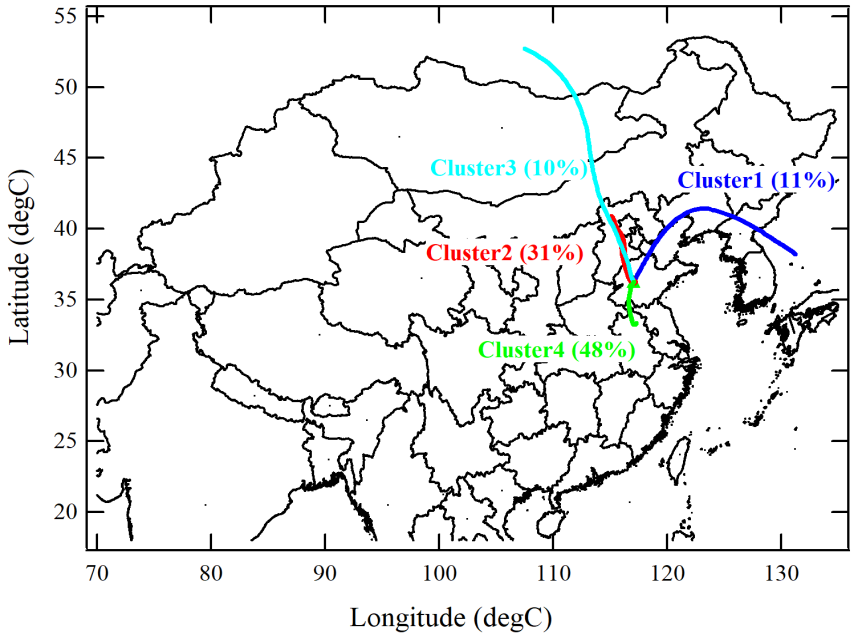

Figure S1. Three-day back-trajectories for Mt. Tai during the sampling period (green triangle: Mt. Tai).

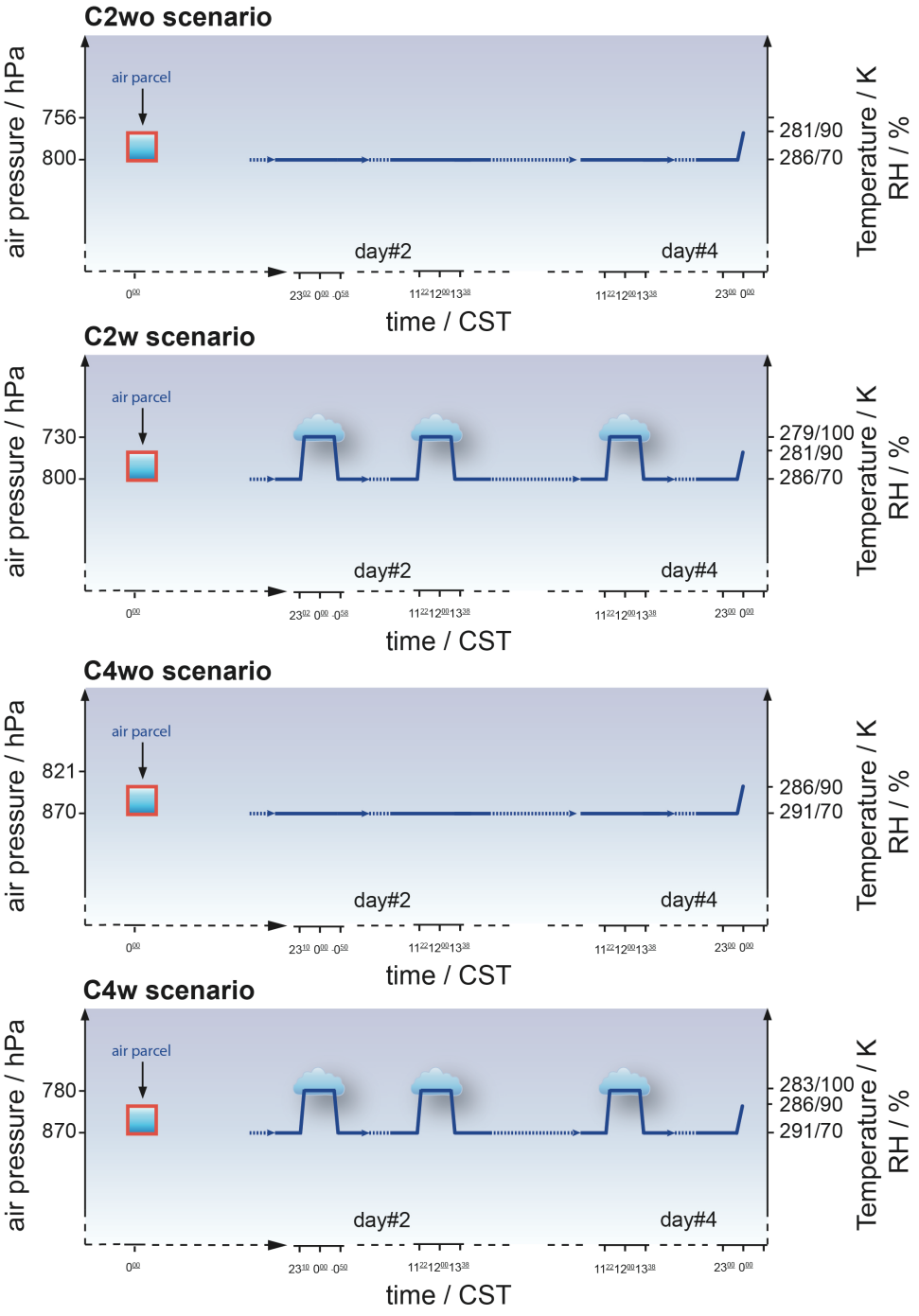

Figure S2. Meteorological data in different scenarios.

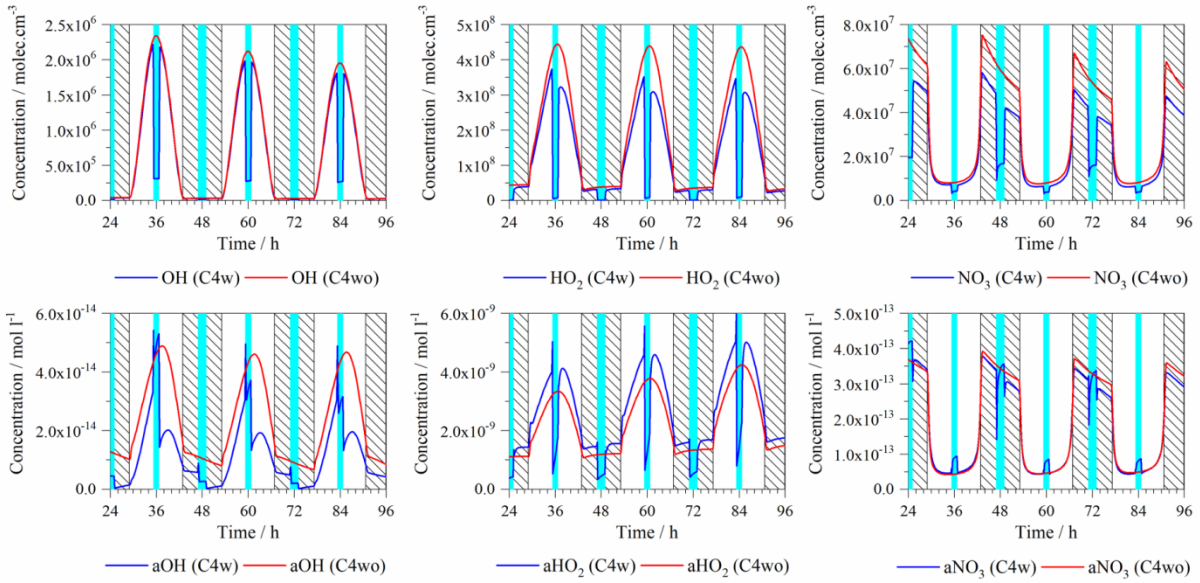

Figure S3. Time series of the modeled radical oxidant concentrations in the C4w and C4wo cases (light blue column: cloud; shadow: night).

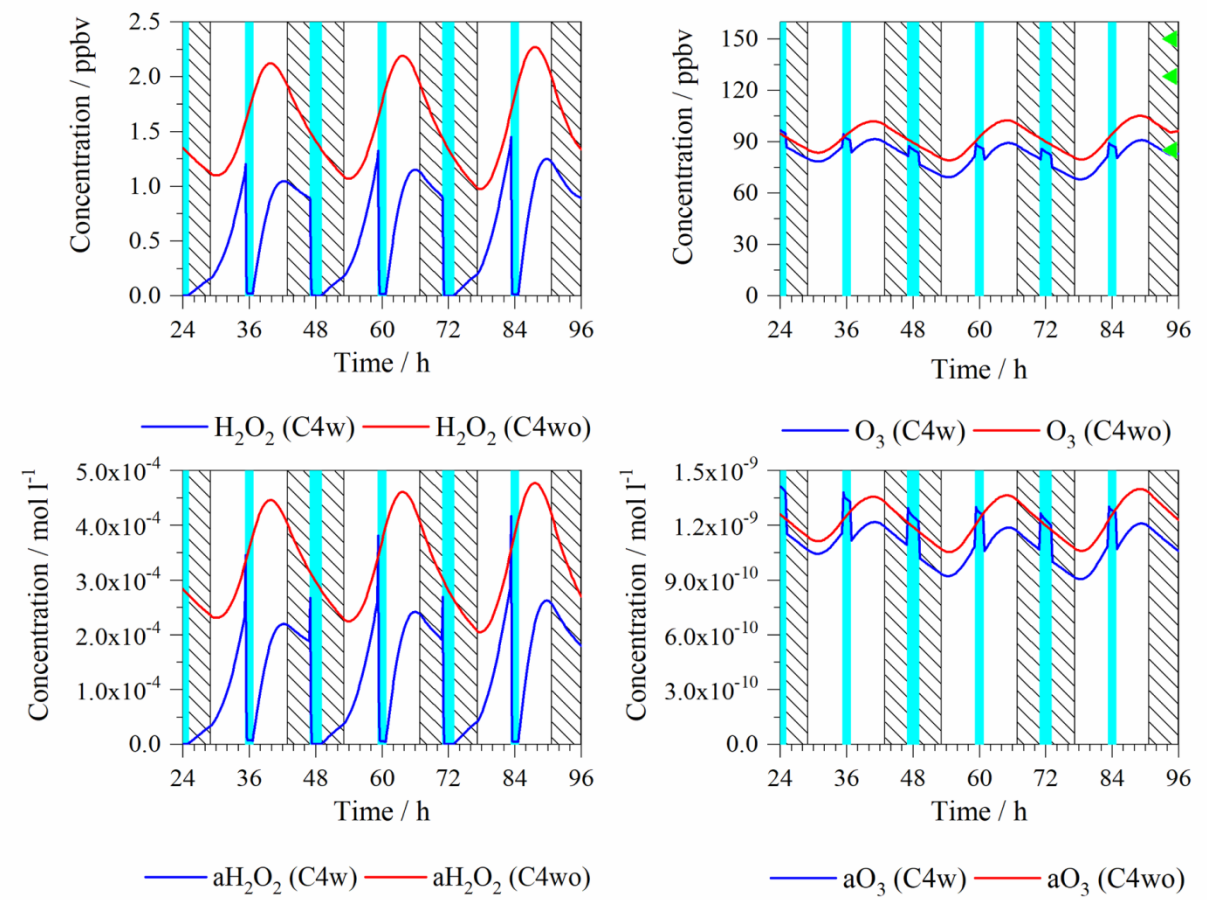

Figure S4. Time series of the modeled non-radical oxidant concentrations in the C4w and C4wo cases (light blue column: cloud; shadow: night; green triangle: maximum (above), average (middle) and minimum (below) value of measured concentration at Mt. Tai).

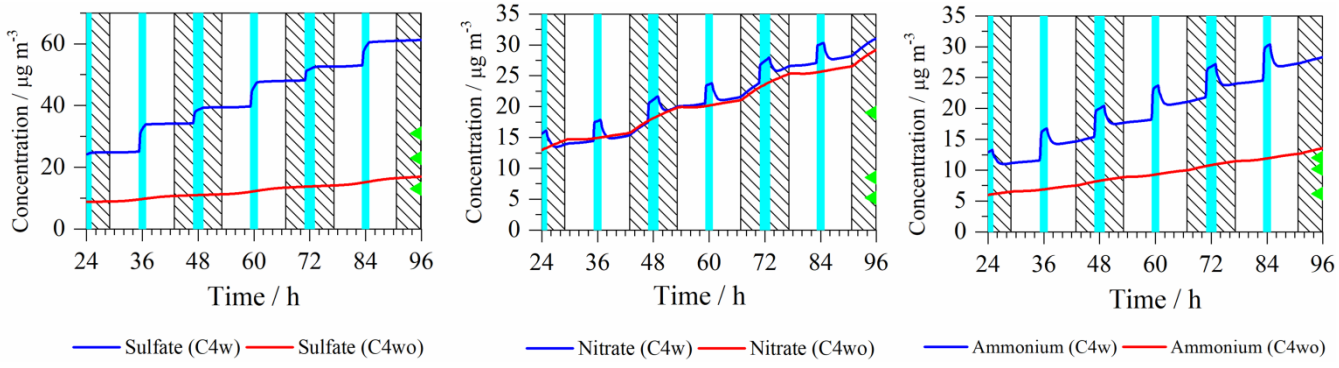

Figure S5. Time series of the modeled concentrations of key secondary inorganic ions in the C4w and C4wo cases (light blue column: cloud; shadow: night; green triangle: maximum (above), average (middle) and minimum (below) value of measured concentrations at Mt. Tai).

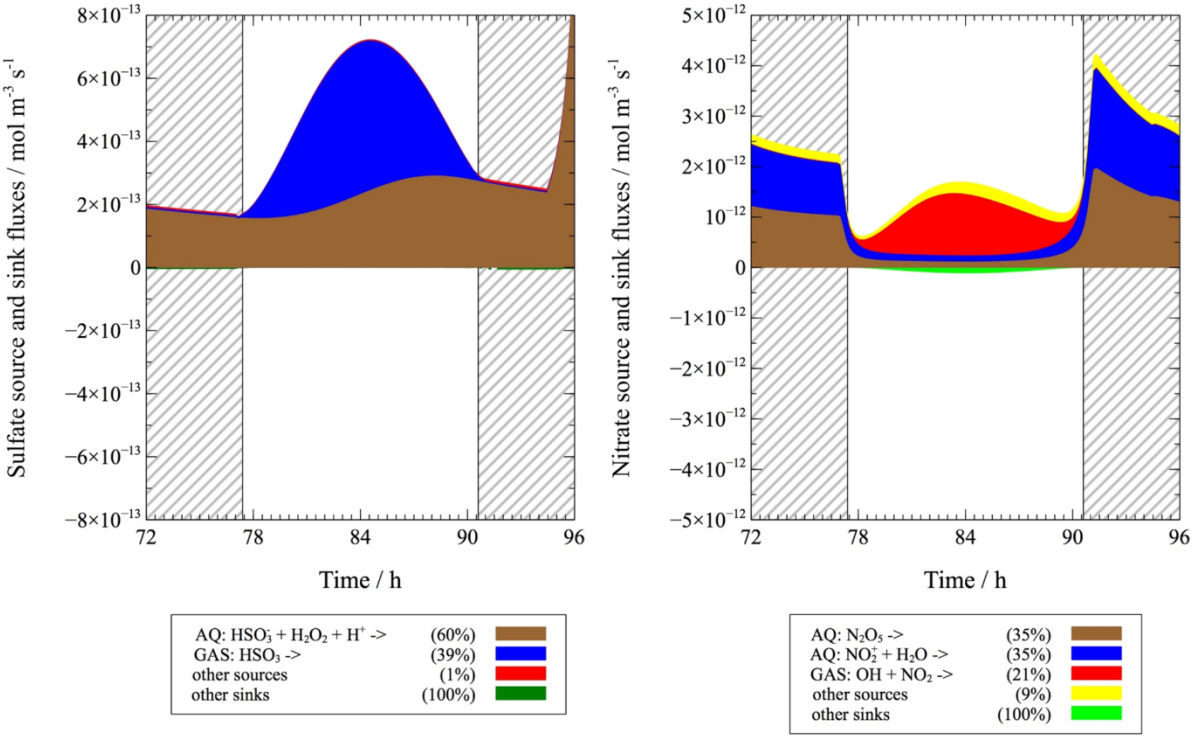

Figure S6. Modeled source and sink fluxes of sulfate (left) and nitrate (right) in the C2wo case (shadow: night).

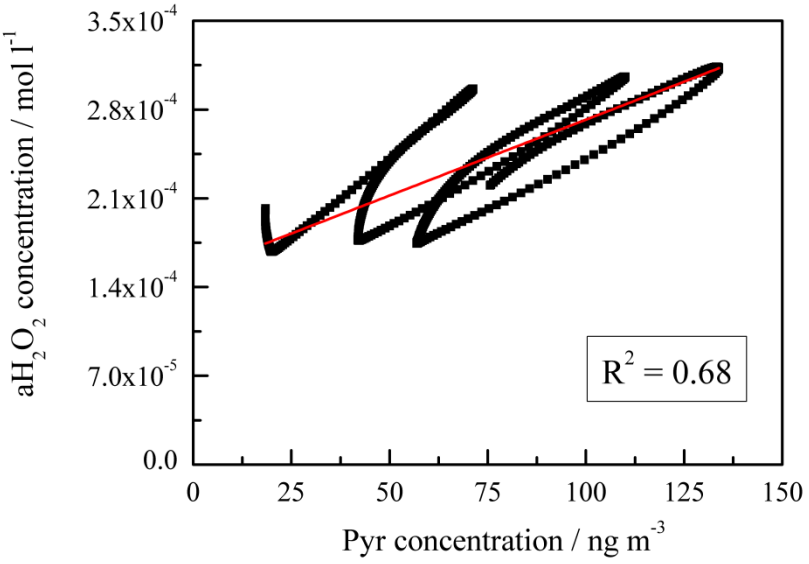

Figure S7. Scatter plot of the concentrations between Pyr and H_2O_2 in the C2wo case.

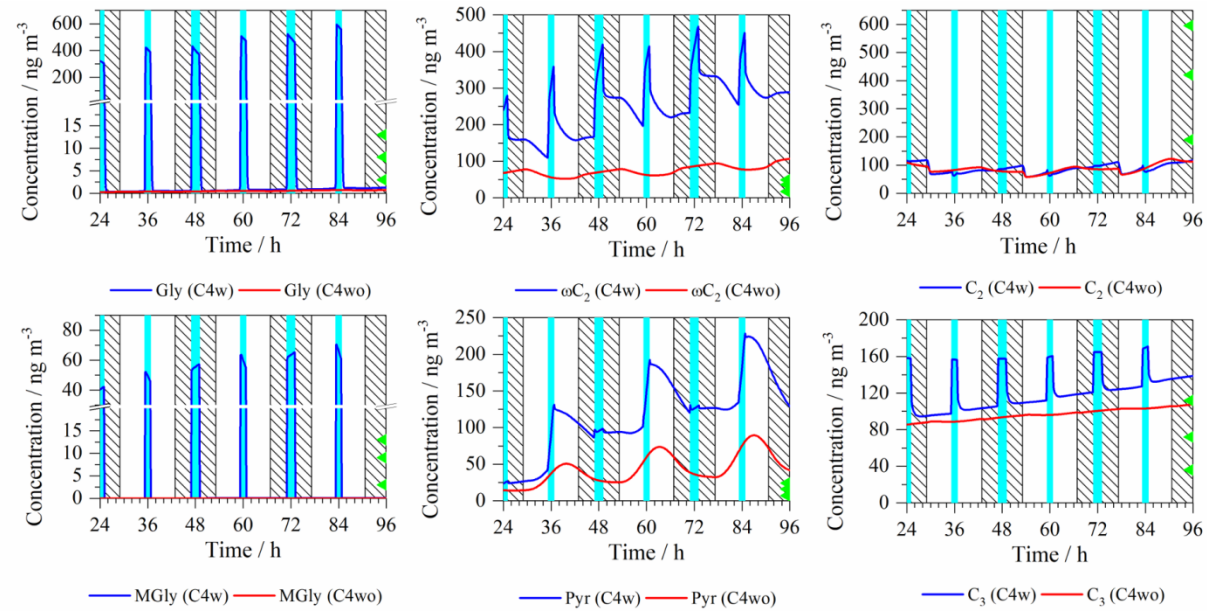

Figure S8. Time series of the modeled concentrations of selected DCRCs in the C4w and C4wo cases (light blue column: cloud; shadow: night; green triangle: maximum (above), average (middle) and minimum (below) value of measured concentration at Mt. Tai).

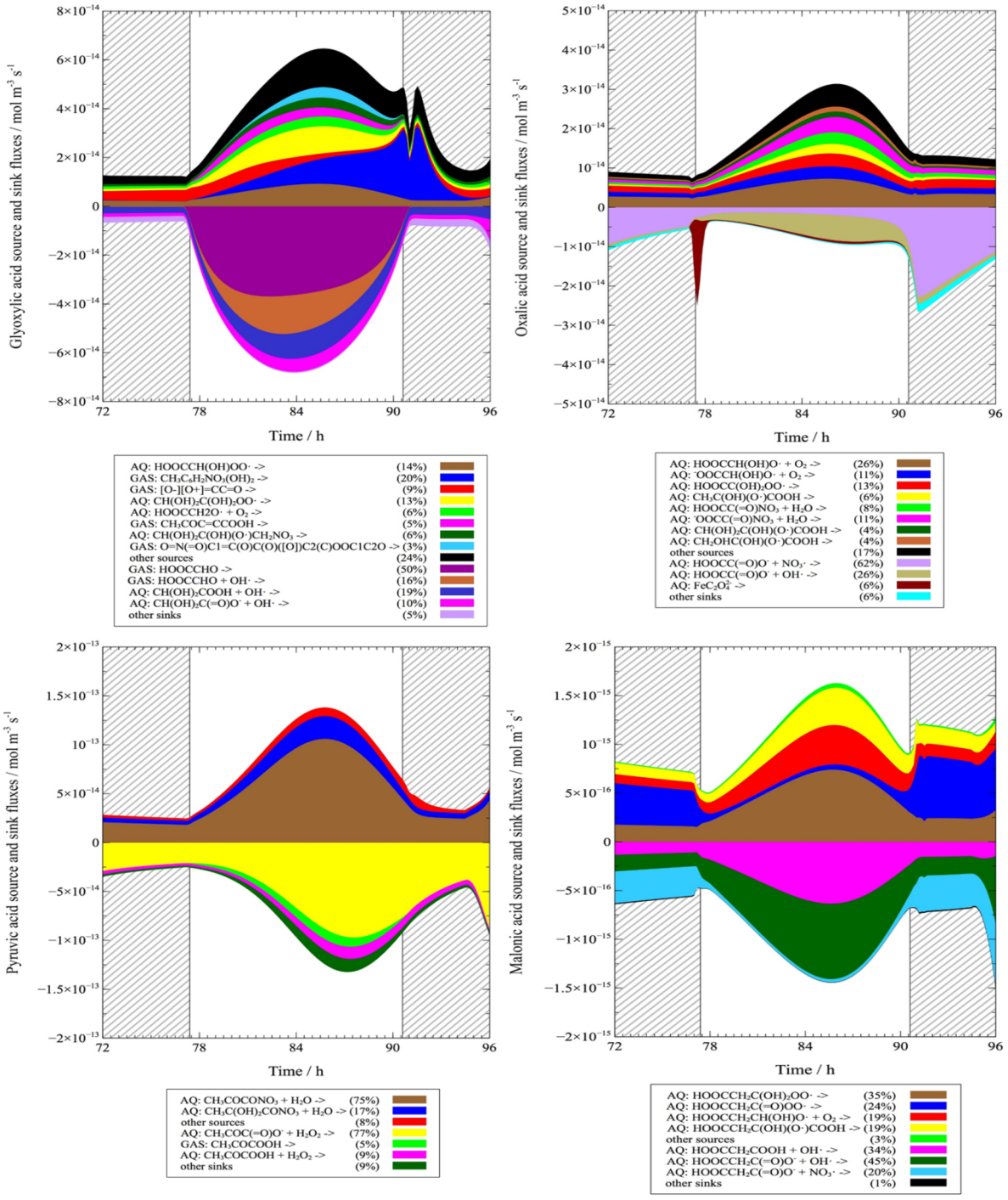

Figure S9. Modeled source and sink fluxes of glyoxylic (above left), oxalic (above right), pyruvic (below left) and malonic (below right) acid in the C2wo case (shadow: night).

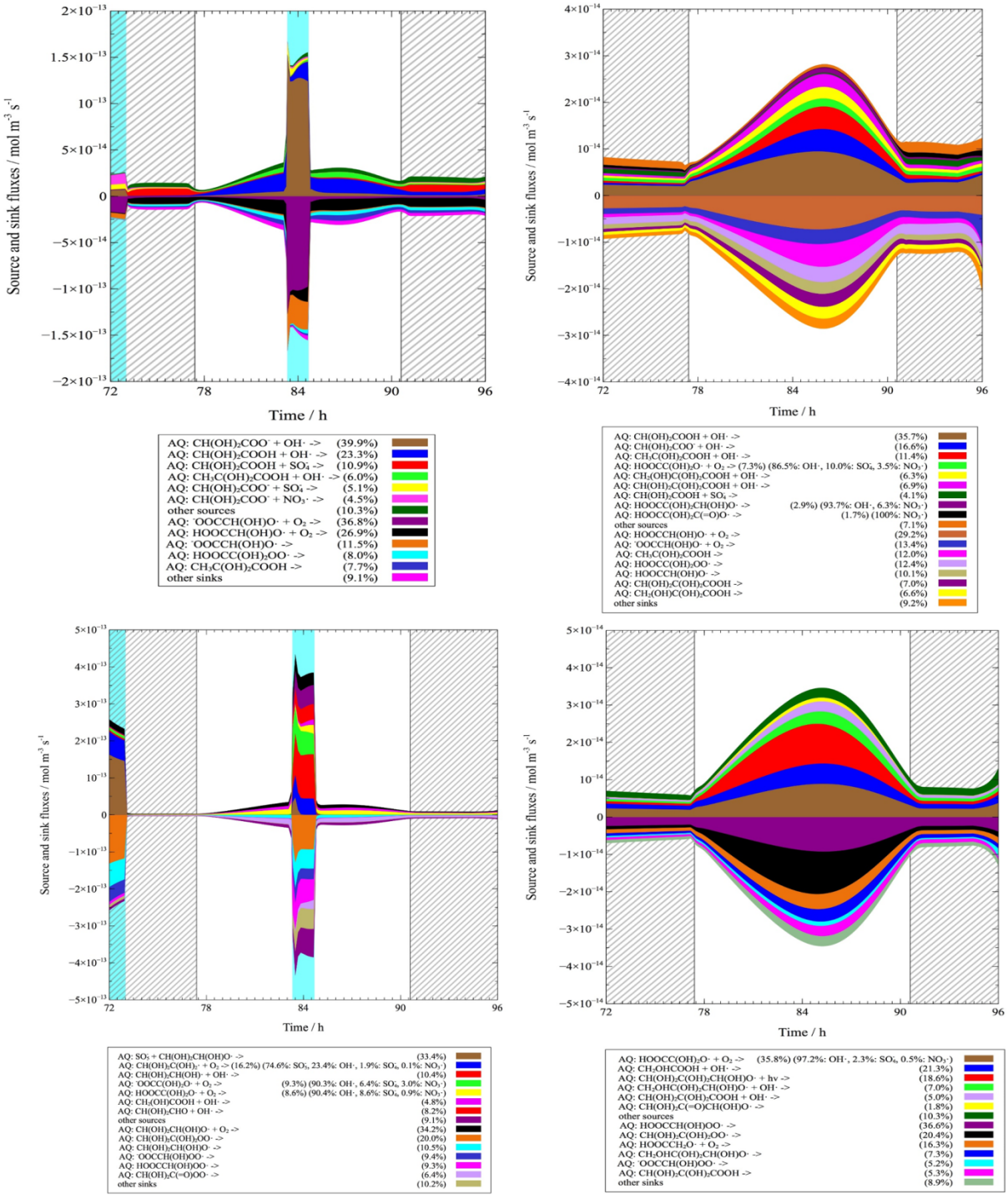

Figure S10. Key oxidants for the source compounds of oxalic (above) and glyoxylic (below) acid in the C2w (left) and C2wo (right) cases.